

1 **Activity of Tricyclic Pyrrolopyrimidine Gyrase B Inhibitor against *Mycobacterium***

2 ***abscessus***

3

4 Abdeldjalil Madani,<sup>a</sup> Dereje A. Negatu,<sup>a,b</sup> Abdellatif El Marrouni,<sup>c</sup> Randy R. Miller,<sup>c</sup> Christopher

5 Boyce,<sup>c</sup> Nicholas Murgolo,<sup>c</sup> Christopher J. Bungard,<sup>c</sup> Matthew D. Zimmerman,<sup>a</sup> Véronique

6 Dartois,<sup>a,d</sup> Martin Gengenbacher,<sup>a,d</sup> David B. Olsen,<sup>c</sup> Thomas Dick<sup>a,d,e,#</sup>

7

8 <sup>a</sup> Center for Discovery and Innovation, Hackensack Meridian Health, Nutley, New Jersey, USA

9 <sup>b</sup> Center for Innovative Drug Development and Therapeutic Trials for Africa (CDT-Africa),

10 Addis Ababa University, Addis Ababa, Ethiopia

11 <sup>c</sup> Merck & Co., Inc., West Point, Pennsylvania, USA

12 <sup>d</sup> Department of Medical Sciences, Hackensack Meridian School of Medicine, Nutley, New

13 Jersey, USA

14 <sup>e</sup> Department of Microbiology and Immunology, Georgetown University, Washington, DC, USA

15

16 Running Title: DNA gyrase inhibitor against *M. abscessus*

17 Keywords: Non-tuberculous mycobacteria, NTM, SPR719, DNA gyrase

18 #Address correspondence to Thomas Dick: [thomas.dick.cdi@gmail.com](mailto:thomas.dick.cdi@gmail.com)

19 **ABSTRACT**

20 Tricyclic pyrrolopyrimidines (TPPs) are a new class of antibacterials inhibiting the ATPase of  
21 DNA gyrase. TPP8, a representative of this class, is active against *Mycobacterium abscessus in*  
22 *vitro*. Spontaneous TPP8 resistance mutations mapped to the ATPase domain of *M. abscessus*  
23 DNA gyrase and the compound inhibited DNA supercoiling activity of recombinant *M.*  
24 *abscessus* enzyme. Further profiling of TPP8 in macrophage and mouse infection studies  
25 demonstrated proof-of-concept activity against *M. abscessus ex vivo* and *in vivo*.

26

27 **MAIN TEXT**

28 *Mycobacterium abscessus* causes difficult-to-cure lung disease (1). Multi-drug regimens are  
29 administered for months to years and typically contain an oral macrolide (clarithromycin,  
30 azithromycin), and intravenously administered amikacin, imipenem and / or cefoxitin or  
31 tigecycline. However, cure rates are unsatisfactory, and treatment refractory patients often  
32 undergo surgical lung resection. To further complicate treatment, the clinical utility of  
33 macrolides against *M. abscessus* is often limited by *erm41*-mediated inducible drug resistance  
34 (2). Given the poor performance of the current regimens, more efficacious drugs are needed. *M.*  
35 *abscessus* drug discovery efforts are hindered by extremely low hit rates in whole cell screens  
36 attempting to identify robust chemical matter starting points (3) (4).

37 *M. abscessus* is intrinsically resistant to many anti-tuberculosis (TB) antibiotics, including all  
38 first line drugs (5). Despite *M. abscessus* resistance to most approved anti-TB drugs, we found  
39 that compound collections of TB actives provide a good source for hit identification (6).  
40 Screening series of advanced TB actives against *M. abscessus* identified several compounds with  
41 *in vivo* activity, including inhibitors of RNA polymerase (7) , ATP synthase (8), Leucyl-tRNA

42 synthetase (9, 10), DNA gyrase (11) and DNA clamp DnaN (12). Expanding on this strategy, we  
43 asked whether the recently identified novel class of tricyclic pyrrolopyrimidines (TPPs (13)),  
44 targeting DNA gyrase in *Mycobacterium tuberculosis* and various other bacteria (14, 15) is  
45 active against *M. abscessus*.

46 DNA gyrase is a validated drug target in mycobacteria. This Type IIA DNA topoisomerase is an  
47 A<sub>2</sub>B<sub>2</sub> heterotetrameric protein that regulates DNA topology (16). Unwinding of DNA during  
48 replication, transcription and recombination introduces positive supercoils into the DNA  
49 molecule that, left unaddressed impedes DNA function. This problem is resolved by DNA  
50 gyrase, which introduces negative supercoils into DNA. To do this, the enzyme generates a DNA  
51 double-strand break, passes a segment of DNA through the break, and subsequently reseals the  
52 DNA molecule (16). The fluoroquinolones target the cleavage-ligation active site of DNA gyrase  
53 formed by subunits A and B, creating stalled enzyme-DNA cleavage complexes (17).

54 Moxifloxacin is used effectively for the treatment of multi-drug resistant TB. However, the  
55 utility of this fluoroquinolone for treatment of *M. abscessus* infections is limited due to  
56 widespread intrinsic resistance (18). Recently, a novel benzimidazole (SPR719, Fig. 1A) entered  
57 early clinical development for mycobacterial lung diseases (19). Benzimidazoles target the  
58 ATPase domain of the DNA gyrase complex, located on its B subunits and required to drive the  
59 catalytic cycle (20), distinct from the fluoroquinolone binding site.

60 Similar to SPR719, TPPs were shown to bind and inhibit the ATPase domain of the gyrase B  
61 subunit in *M. tuberculosis* (14). To determine whether this novel class of inhibitors is active  
62 against *M. abscessus*, the minimum inhibitory concentration (MIC) of a representative TPP  
63 compound (TPP8, compound #8 in (15) and Fig. 1A (21, 22), provided by Merck & Co., Inc.,  
64 Kenilworth, NJ, USA was determined. Dose-response curves were established in Middlebrook

65 7H9 medium using the microbroth dilution method with OD<sub>600</sub> as readout as described  
66 previously (23) . TPP8 retained activity against reference strains from culture collections  
67 representing the subspecies of *M. abscessus*, including the type-strain *M. abscessus* subsp.  
68 *abscessus* ATCC19977, and a panel of clinical isolates, including *M. abscessus* subsp. *abscessus*  
69 K21, used in our mouse model of infection (Table 1). With growth inhibitory activity in the 0.02  
70 to 0.2 μM range, TPP8 exhibited a markedly higher potency than SPR719 or moxifloxacin  
71 (Sigma-Aldrich), both showing MICs in the low micromolar range (Table 1). These results  
72 indicate that TPP8 is broadly active against the *M. abscessus* complex and displays potent  
73 antimycobacterial activity.

74 To confirm that TPP8 exerts anti-*M. abscessus* whole cell activity via inhibition of gyrase B,  
75 spontaneous resistant mutants in *M. abscessus* ATCC19977 were selected on Middlebrook 7H10  
76 agar as described previously (23). The agar MIC of TPP8 (lowest drug concentration that  
77 suppresses emergence of colonies when plating 10<sup>4</sup> CFU on 7H10) was 0.64 μM as determined  
78 by the agar dilution method according to the CLSI protocol (24). To isolate spontaneous TPP8  
79 resistant mutants, a total of 10<sup>9</sup> CFU was plated on ten 30 mL agar plates containing 4x agar  
80 MIC, yielding one colony. TPP8 resistance was confirmed by re-streaking the colony on agar  
81 containing the same TPP8 concentration. The experiment was repeated once with an  
82 independently grown culture yielding a second TPP8 resistant *M. abscessus* strain. The broth  
83 MIC was similar for both mutants, 75-fold higher than the wild-type (Table 2). Susceptibility to  
84 moxifloxacin and clarithromycin (Sigma-Aldrich) was not affected, reducing the likelihood of a  
85 nonspecific mechanism of resistance (Table 2). Sanger sequencing of the gyrase B coding  
86 sequence, using primers GyrB-1 (GGCGTGGTGACGAGTTTAAAG), GyrB-2  
87 (GAGATCTTCGAGACCACCACCTA), GyrB-3 (GCAAGAGTGCCACCGATATC) and

88 GyrB-4 (GTAAGTACGACGGCACAACG) (Genewiz Inc.), showed that both resistant strains  
89 harbored a C506A (Thr169Asn) missense mutation, located in the ATPase domain (20) (Table  
90 2). Interestingly, the same amino acid substitution in the *M. abscessus* gyrase B ATPase domain  
91 was previously shown to confer resistance to SPR719 (25). Indeed, cross resistance studies  
92 showed that the two TPP8 resistant *M. abscessus* ATCC19977 strains were resistant to SPR719  
93 and that the previously isolated SPR719 resistant *M. abscessus* ATCC19977 strain harboring the  
94 C506A missense mutation (25) was resistant to TPP8 (Table 2). To confirm that the observed  
95 missense mutation in *gyrB* indeed causes resistance, the C506A allele of *gyrB* was  
96 overexpressed in wild-type *M. abscessus* ATCC19977 using a custom synthesized (Genewiz  
97 Inc.) pMV262-*hsp60*-based expression system for *gyrBA* as described previously (23). The strain  
98 expressing the mutant enzyme showed resistance to both TPP8 and SPR719, confirming GyrB as  
99 the intracellular target (Table 2). To directly demonstrate that TPP8 inhibits *M. abscessus* DNA  
100 gyrase activity, *in vitro* DNA supercoiling inhibition studies were performed using recombinant  
101 *M. abscessus* enzyme and plasmid pBR322 (Inspiralis) as substrate, as described (23). The  
102 results demonstrate concentration-dependent enzyme inhibition by TPP8 (Fig. 1B,C). Consistent  
103 with the improved whole cell inhibitory potency of TPP8 compared to SPR719, the compound  
104 showed higher potency against the target with a half maximal inhibitory concentration (IC<sub>50</sub>) of  
105 0.3 μM vs. 1 μM for SPR719. Together, these results provide genetic and biochemical evidence  
106 that TPP8 retained DNA gyrase B as its target in *M. abscessus*.

107 To further characterize *in vitro* and *ex vivo* anti-*M. abscessus* activities of TPP8, kill experiments  
108 against *M. abscessus* ATCC19977 growing in Middlebrook 7H9 broth were performed and the  
109 inhibitory potency of TPP8 against bacteria growing intracellularly in infected THP-1 derived

110 macrophages (ATCC TIB-202) was determined (26). TPP8 was largely bacteriostatic in broth  
111 culture (Fig. 2A) and inhibited growth of intracellular bacteria (Fig. 2B).

112 To determine whether the attractive *in vitro* and *ex vivo* activities of TPP8 translate into *in vivo*  
113 efficacy, an immunodeficient murine model developed by our group was utilized (7), in which  
114 mice are infected with the *M. abscessus* clinical isolate K21 (TPP8 MIC = 0.06  $\mu$ M, Table 1) to  
115 generate a sustained infection resulting in a largely constant bacterial lung burden, thus allowing  
116 the effects of drugs to be evaluated (7). As TPP8 lacks robust oral bioavailability (15), the  
117 plasma concentration-time profile upon intraperitoneal administration in CD-1 mice (Charles  
118 River Laboratories) was determined. TPP8 plasma concentrations were measured by liquid  
119 chromatography-coupled tandem mass spectrometry. The *in vivo* pharmacokinetic analysis  
120 revealed that a dose of 25 mg/kg retains concentrations above the MIC of *M. abscessus* K21 for  
121 the 24h dosing interval (Fig. 3A). 8-week old female NOD.CB17-Prkdc<sup>scid</sup>/NCrCrl mice (NOD  
122 SCID; Charles River Laboratories) were infected by intranasal delivery of 10<sup>6</sup> CFU as described  
123 previously (7). TPP8 was administered intraperitoneally once daily for 10 consecutive days at 25  
124 and 12.5 mg/kg, starting one day post-infection. Two comparator agents were used in the  
125 efficacy study: the phosphate prodrug form of SPR719, SPR720 (20), administered orally at 100  
126 mg/kg, and moxifloxacin administered orally at 200 mg/kg (11), the efficacious dose in TB  
127 mouse models (20). Clarithromycin as positive control was administered orally at 250 mg/kg  
128 (11). All mice were euthanized 24h after the last dose, and bacterial load in the lungs and spleen  
129 was determined by plating serial dilutions of organ homogenates on Middlebrook 7H11 agar. All  
130 experiments involving live animals were approved by the Institutional Animal Care and Use  
131 Committee of the Center for Discovery and Innovation, Hackensack Meridian Health. As  
132 expected, treatment with vehicle alone did not affect the bacterial lung burden ('D11 DF', Fig.

133 3B). Compared to the vehicle control, treatment with 25 mg/kg TPP8 reduced lung CFUs ~20-  
134 fold. The comparators SPR720 and moxifloxacin, and the positive control clarithromycin  
135 reduced the lung burden to a similar degree (Fig. 3B). CFU reduction in the spleen followed a  
136 similar pattern (Fig. 3B). Thus, TPP8 is efficacious in a mouse model of *M. abscessus* infection.

137 In conclusion, the tricyclic pyrrolopyrimidine TPP8 is active against *M. abscessus in vitro, ex*  
138 *vivo* and in a mouse model of infection and exerts its antimicrobial activity by inhibiting the B  
139 subunit of DNA gyrase. This work adds a new lead compound to the preclinical *M. abscessus*  
140 drug pipeline and provides an attractive chemical starting point for an optimization program  
141 aiming at improving oral bioavailability. The demonstration that yet another TB active displays  
142 anti-*M. abscessus* activity supports the strategy of exploiting chemical matter shown to be active  
143 against *M. tuberculosis* to accelerate *de novo* drug discovery for *M. abscessus*.

144

## 145 **ACKNOWLEDGMENTS**

146 We are grateful to Wei Chang Huang (Taichung Veterans General Hospital, Taichung, Taiwan)  
147 for providing *M. abscessus* Bamboo, to Jeanette W.P. Teo (Department of Laboratory Medicine,  
148 National University Hospital, Singapore) for providing the collection of *M. abscessus* clinical M  
149 isolates, and to Sung Jae Shin (Department of Microbiology, Yonsei University College of  
150 Medicine, Seoul, South Korea) and Won-Jung Koh (Division of Pulmonary and Critical Care  
151 Medicine, Samsung Medical Center, Seoul, South Korea) for providing *M. abscessus* K21. We  
152 thank Wassihun Aragaw (Center for Discovery and Innovation, Hackensack Meridian Health,  
153 Nutley, New Jersey, USA) for providing the SPR719 resistant *M. abscessus* isolate. Research  
154 reported in this work was supported by the National Institute of Allergy and Infectious Diseases  
155 of the National Institutes of Health under Award Number R01AI132374. The content is solely

156 the responsibility of the authors and does not necessarily represent the official views of the  
157 National Institutes of Health.

158

## 159 **AUTHOR CONTRIBUTIONS**

160 Investigation: A.M., D.A.N., A.E.M., R.R.M., C.J.B., M.D.Z., M.G.; Materials: A.E.M.; Writing  
161 - Original Draft: A.M., D.A.N., T.D.; Writing - Review & Editing: all authors; Funding  
162 Acquisition: T.D., D.B.O.; Supervision: C.B., N.M., V.D., M.G., D.B.O., T.D.

163

## 164 **CONFLICT OF INTEREST STATEMENT**

165 The authors declare no commercial or financial relationships that could be construed as a  
166 potential conflict of interest. A.E.M, R.R.M., C.B., N.M., C.J.B. and D.B.O. are employees of  
167 Merck Sharp & Dohme Corp., a subsidiary of Merck & Co., Inc., Kenilworth, NJ, USA.

## 168 **REFERENCES**

- 169 1. Johansen MD, Herrmann JL, Kremer L. 2020. Non-tuberculous mycobacteria and the rise  
170 of Mycobacterium abscessus. *Nat Rev Microbiol* 18:392-407.
- 171 2. Griffith DE, Daley CL. 2022. Treatment of Mycobacterium abscessus Pulmonary  
172 Disease. *Chest* 161:64-75.
- 173 3. Egorova A, Jackson M, Gavriilyuk V, Makarov V. 2021. Pipeline of anti-Mycobacterium  
174 abscessus small molecules: Repurposable drugs and promising novel chemical entities.  
175 *Med Res Rev* 41:2350-2387.
- 176 4. Wu ML, Aziz DB, Dartois V, Dick T. 2018. NTM drug discovery: status, gaps and the  
177 way forward. *Drug Discov Today* 23:1502-1519.



- 178 5. Luthra S, Rominski A, Sander P. 2018. The Role of Antibiotic-Target-Modifying and  
179 Antibiotic-Modifying Enzymes in Mycobacterium abscessus Drug Resistance. Front  
180 Microbiol 9:2179.
- 181 6. Low JL, Wu ML, Aziz DB, Laleu B, Dick T. 2017. Screening of TB Actives for Activity  
182 against Nontuberculous Mycobacteria Delivers High Hit Rates. Front Microbiol 8:1539.
- 183 7. Dick T, Shin SJ, Koh WJ, Dartois V, Gengenbacher M. 2020. Rifabutin Is Active against  
184 Mycobacterium abscessus in Mice. Antimicrob Agents Chemother 64(2):e01943-19.
- 185 8. Sarathy JP, Ganapathy US, Zimmerman MD, Dartois V, Gengenbacher M, Dick T. 2020.  
186 TBAJ-876, a 3,5-Dialkoxypyridine Analogue of Bedaquiline, Is Active against  
187 Mycobacterium abscessus. Antimicrob Agents Chemother 64(4):e02404-19.
- 188 9. Ganapathy US, Del Rio RG, Cacho-Izquierdo M, Ortega F, Lelievre J, Barros-Aguirre D,  
189 Lindman M, Dartois V, Gengenbacher M, Dick T. 2021. A Leucyl-tRNA Synthetase  
190 Inhibitor with Broad-Spectrum Anti-Mycobacterial Activity. Antimicrob Agents  
191 Chemother doi:10.1128/AAC.02420-20.
- 192 10. Ganapathy US, Gengenbacher M, Dick T. 2021. Epetraborole Is Active against  
193 Mycobacterium abscessus. Antimicrob Agents Chemother 65:e0115621.
- 194 11. Ganapathy US, Del Rio RG, Cacho-Izquierdo M, Ortega F, Lelievre J, Barros-Aguirre D,  
195 Aragaw WW, Zimmerman MD, Lindman M, Dartois V, Gengenbacher M, Dick T. 2021.  
196 A Mycobacterium tuberculosis NBTI DNA Gyrase Inhibitor Is Active against  
197 Mycobacterium abscessus. Antimicrob Agents Chemother 65:e0151421.
- 198 12. Aragaw WW, Roubert C, Fontaine E, Lagrange S, Zimmerman MD, Dartois V,  
199 Gengenbacher M, Dick T. 2022. Cyclohexyl-griselimycin Is Active against  
200 Mycobacterium abscessus in Mice. Antimicrob Agents Chemother 66:e0140021.

- 201 13. Tari LW, Li X, Trzoss M, Bensen DC, Chen Z, Lam T, Zhang J, Lee SJ, Hough G,  
202 Phillipson D, Akers-Rodriguez S, Cunningham ML, Kwan BP, Nelson KJ, Castellano A,  
203 Locke JB, Brown-Driver V, Murphy TM, Ong VS, Pillar CM, Shinabarger DL, Nix J,  
204 Lightstone FC, Wong SE, Nguyen TB, Shaw KJ, Finn J. 2013. Tricyclic GyrB/ParE  
205 (TriBE) inhibitors: a new class of broad-spectrum dual-targeting antibacterial agents.  
206 PLoS One 8:e84409.
- 207 14. Henderson SR, Stevenson CEM, Malone B, Zholnerovych Y, Mitchenall LA, Pichowicz  
208 M, McGarry DH, Cooper IR, Charrier C, Salisbury AM, Lawson DM, Maxwell A. 2020.  
209 Structural and mechanistic analysis of ATPase inhibitors targeting mycobacterial DNA  
210 gyrase. *J Antimicrob Chemother* 75:2835-2842.
- 211 15. Durcik M, Tomasic T, Zidar N, Zega A, Kikelj D, Masic LP, Ilas J. 2019. ATP-  
212 competitive DNA gyrase and topoisomerase IV inhibitors as antibacterial agents. *Expert*  
213 *Opin Ther Pat* 29:171-180.
- 214 16. McKie SJ, Neuman KC, Maxwell A. 2021. DNA topoisomerases: Advances in  
215 understanding of cellular roles and multi-protein complexes via structure-function  
216 analysis. *Bioessays* 43:e2000286.
- 217 17. Aldred KJ, Kerns RJ, Osheroff N. 2014. Mechanism of quinolone action and resistance.  
218 *Biochemistry* 53:1565-74.
- 219 18. Kim SY, Jhun BW, Moon SM, Shin SH, Jeon K, Kwon OJ, Yoo IY, Huh HJ, Ki CS, Lee  
220 NY, Shin SJ, Daley CL, Suh GY, Koh WJ. 2018. Mutations in *gyrA* and *gyrB* in  
221 Moxifloxacin-Resistant *Mycobacterium avium* Complex and *Mycobacterium abscessus*  
222 Complex Clinical Isolates. *Antimicrob Agents Chemother* 62(9):e00527-18.

- 223 19. Talley AK, Thurston A, Moore G, Gupta VK, Satterfield M, Manyak E, Stokes S, Dane  
224 A, Melnick D. 2021. First-in-Human Evaluation of the Safety, Tolerability, and  
225 Pharmacokinetics of SPR720, a Novel Oral Bacterial DNA Gyrase (GyrB) Inhibitor for  
226 Mycobacterial Infections. *Antimicrob Agents Chemother* 65:e0120821.
- 227 20. Locher CP, Jones SM, Hanzelka BL, Perola E, Shoen CM, Cynamon MH, Ngwane AH,  
228 Wiid IJ, van Helden PD, Betoudji F, Nuermberger EL, Thomson JA. 2015. A novel  
229 inhibitor of gyrase B is a potent drug candidate for treatment of tuberculosis and  
230 nontuberculosis mycobacterial infections. *Antimicrob Agents Chemother* 59:1455-65.
- 231 21. Finn F, Tari LW, Chen Z, Zhang J, Phillipson D, Lee SJ, Trzoss M, Bensen D, Li X,  
232 Teng T, Ong V, Borchardt AJ, TT. L. 19 March 2015. Tricyclic gyrase inhibitors. patent  
233 WO 2015/038661 A1.
- 234 22. Bensen D, Borchardt A, Chen Z, Finn JM, Lam TT, Lee SJ, Li X, Tari LW, Teng M,  
235 Trzoss M, Zhang J, Jung ME, Lightstone FC, Wong SE, TB. N. 20 March 2014. Tricyclic  
236 gyrase inhibitors for use as antibacterial agents. patent WO 2014/043271 A1.
- 237 23. Negatu DA, Beuchel A, Madani A, Alvarez N, Chen C, Aragaw WW, Zimmerman MD,  
238 Laleu B, Gengenbacher M, Dartois V, Imming P, Dick T. 2021. Piperidine-4-  
239 Carboxamides Target DNA Gyrase in Mycobacterium abscessus. *Antimicrob Agents*  
240 *Chemother* 65:e0067621.
- 241 24. CLSI. 2018. Methods for dilution antimicrobial susceptibility tests for bacteria that grow  
242 aerobically, Wayne, PA.
- 243 25. Aragaw WW, Cotroneo N, Stokes S, Pucci M, Critchley I, Gengenbacher M, Dick T.  
244 2022. In Vitro Resistance against DNA Gyrase Inhibitor SPR719 in Mycobacterium  
245 avium and Mycobacterium abscessus. *Microbiol Spectr* 10:e0132121.

- 246 26. Kaya F, Ernest JP, LoMauro K, Gengenbacher M, Madani A, Aragaw WW, Zimmerman  
247 MD, Sarathy JP, Alvarez N, Daudelin I, Wang H, Lanni F, Weiner DM, Via LE, Barry  
248 CE, 3rd, Olivier KN, Dick T, Podell BK, Savic RM, Dartois V. 2022. A Rabbit Model to  
249 Study Antibiotic Penetration at the Site of Infection for Nontuberculous Mycobacterial  
250 Lung Disease: Macrolide Case Study. *Antimicrob Agents Chemother* 66:e0221221.
- 251 27. Yee M, Klinzing D, Wei JR, Gengenbacher M, Rubin EJ, Dick T. 2017. Draft Genome  
252 Sequence of *Mycobacterium abscessus* Bamboo. *Genome Announc* 5(20):e00388-17.
- 253 28. Aziz DB, Low JL, Wu ML, Gengenbacher M, Teo JW, Dartois V, Dick T. 2017.  
254 Rifabutin Is Active Against *Mycobacterium abscessus* Complex. *Antimicrob Agents*  
255 *Chemother* doi:10.1128/AAC.00155-17.
- 256 29. Nash KA, Brown-Elliott BA, Wallace RJ, Jr. 2009. A novel gene, *erm(41)*, confers  
257 inducible macrolide resistance to clinical isolates of *Mycobacterium abscessus* but is  
258 absent from *Mycobacterium chelonae*. *Antimicrob Agents Chemother* 53:1367-76.

259 **TABLES**

260

261 **Table 1.** Activity of TPP8 against *M. abscessus* complex.

262

<i>M. abscessus</i> strains	<i>erm41</i> sequevar <sup>c</sup>	CLR susceptibility	MIC <sup>a</sup> [μM]			
			TPP8 <sup>d</sup>	SPR719 <sup>d</sup>	MXF <sup>d</sup>	CLR <sup>d</sup>
<b>Reference strains</b>						
subsp. <i>abscessus</i> ATCC19977	T28	Resistant	0.02	1.5	3	3
subsp. <i>bolletii</i> CCUG50184T	T28	Resistant	0.2	1.5	3	6
subsp. <i>massiliense</i> CCUG48898T	Deletion	Sensitive	0.1	3	6	0.2
<b>Clinical isolates<sup>b</sup></b>						
subsp. <i>abscessus</i> Bamboo	C28	Sensitive	0.2	1.5	6	0.4
subsp. <i>abscessus</i> K21	C28	Sensitive	0.06	1.5	3	0.2
subsp. <i>abscessus</i> M9	T28	Resistant	0.06	3	6	6
subsp. <i>abscessus</i> M199	T28	Resistant	0.02	3	3	6
subsp. <i>abscessus</i> M337	T28	Resistant	0.02	1.5	3	6
subsp. <i>abscessus</i> M404	C28	Sensitive	0.06	3	6	0.2
subsp. <i>abscessus</i> M421	T28	Resistant	0.06	1.5	3	3
subsp. <i>bolletii</i> M232	T28	Resistant	0.04	3	3	6
subsp. <i>bolletii</i> M506	C28	Sensitive	0.2	6	6	0.4
subsp. <i>massiliense</i> M111	Deletion	Sensitive	0.2	6	3	0.4

263

264 <sup>a</sup>MIC values are the mean of three independent experiments.

265 <sup>b</sup>*M. abscessus* Bamboo (27), K21 (7), M strains (28) were reported previously.

266 <sup>c</sup>*erm41*, ribosome methylase gene conferring inducible clarithromycin (CLR) resistance. ‘C28’

267 and ‘deletion’ sequevars are inactive *erm41* alleles and susceptible to CLR. The ‘T28’ sequevar

268 is functional and confers inducible resistance against CLR (29).

269 <sup>d</sup>TPP8, Tricyclic pyrrolopyrimidine compound 8; SPR719, benzimidazole Gyrase B ATPase

270 inhibitor; MXF, moxifloxacin; CLR, clarithromycin (assay control).

271 **Table 2.** Characterization of TPP8-resistant *M. abscessus* ATCC19977.

<i>M. abscessus</i> ATCC19977	MIC <sup>a</sup> (μM)				GyrB mutation
	TPP8 <sup>e</sup>	SPR719 <sup>e</sup>	MXF <sup>e</sup>	CLR <sup>e</sup>	
Wildtype	0.02	1.5	3	3	wt
TPP8 <sup>R</sup> -1 <sup>b</sup>	1.5	>25 <sup>f</sup>	3	1.5	Thr169Asn
TPP8 <sup>R</sup> -2 <sup>b</sup>	1.5	>25 <sup>f</sup>	1.5	1.5	Thr169Asn
SPR <sup>R</sup> -L1.2 <sup>c</sup>	3	>25 <sup>f</sup>	3	2	Thr169Asn
pMV262/ <i>hsp60 gyrB</i> *A <sup>d</sup>	0.4	12.5	1.5	3	wt
pMV262/ <i>hsp60</i> empty <sup>d</sup>	0.02	1.5	3	3	wt

272

273 <sup>a</sup> MIC values are the mean of three independent experiments.

274 <sup>b</sup> independently isolated TPP8 resistant mutant strains.

275 <sup>c</sup> SPR719 resistant mutant strain reported previously (25).

276 <sup>d</sup> wild-type strain expressing the DNA gyrase B\* and A subunits carried by pMV262 under  
277 control of *hsp60* (23) with Gyrase B\* harboring a Thr169Asn amino acid substitution.

278 ‘pMV262/*hsp60* empty’, wild-type strain harboring the pMV262 expression system without  
279 gyrase genes inserted.

280 <sup>e</sup> TPP8, Tricyclic pyrrolopyrimidine compound 8; SPR719, benzimidazole Gyrase B ATPase  
281 inhibitor; MXF, moxifloxacin; CLR, clarithromycin (assay control).

282 <sup>f</sup> concentrations >25 μM could not be tested because of limited solubility of the compound (25).

283

284 **FIGURE LEGENDS**

285  
286 **Figure 1.** Structure and DNA gyrase inhibition activity of TPP8. **(A)** Structure of TPP8 and  
287 SPR719 (15, 20). **(B)** Effect of TPP8 and comparator compounds on the DNA supercoiling  
288 activity of recombinant *M. abscessus* ATCC19977 DNA gyrase. Relaxed pBR322 plasmid was  
289 used as substrate to measure the effect of compounds on the supercoiling activity of *M.*  
290 *abscessus* DNA gyrase as described (23). The conversion of relaxed (R) into supercoiled (SC)  
291 plasmid by DNA gyrase was visualized by agarose gel electrophoresis. OC: open circular  
292 plasmid. Lane 13, Gyrase -: reaction mix without added enzyme showing unaltered substrate.  
293 Lane 12, Gyrase +: reaction mix with added enzyme (without drug) showing conversion of  
294 relaxed plasmid into its supercoiled form. Lanes 1 to 11 show the effect of decreasing drug  
295 concentrations. The concentration ranges are as follows: TPP8: 1.5, 0.75, 0.37, 0.18, 0.09, 0.04,  
296 0.02, 0.01, 0.005, 0.002, and 0.001  $\mu\text{M}$ . SPR719, MXF and CLR: 50, 25, 12.5, 6.25, 3.12, 1.56,  
297 0.78, 0.39, 0.19, 0.09, and 0.04  $\mu\text{M}$ . The experiments were repeated three times independently  
298 yielding similar results and a representative example is shown. **(C)** Quantitative inhibition of  
299 DNA gyrase supercoiling activity by TPP8 and comparator drugs. The bands obtained from the  
300 three experiments represented in **(B)** were quantified by the Invitrogen iBright™ FL1000  
301 imaging system to determine half-maximal inhibitory concentrations ( $\text{IC}_{50}$ ) as described  
302 previously (23). Means and standard deviations are shown. TPP8 inhibited DNA gyrase with an  
303  $\text{IC}_{50}$  of 0.3  $\mu\text{M}$ . SPR719 and MXF inhibited the enzyme with an  $\text{IC}_{50}$  of 1  $\mu\text{M}$  and 3  $\mu\text{M}$ ,  
304 respectively (23).  $\text{IC}_{50}$  derived from **(C)** are indicated by asterisks in **(B)**. CLR, included as  
305 negative control, did not affect the supercoiling activity of the enzyme.

306

307 **Figure 2.** Activity of TPP8 against *M. abscessus* growing in broth and in THP-1 derived  
308 macrophages. **(A)** To determine whether TPP8 displays bactericidal activity *in vitro*, 1 mL  
309 cultures of *M. abscessus* ATCC19977 growing in Middlebrook 7H9 in tubes (11) were treated  
310 with MIC multiples of TPP8, SPR719, moxifloxacin (MXF), or clarithromycin (CLR). CFU  
311 were enumerated by plating samples on Middlebrook 7H10 agar. The growth kinetics of drug  
312 free controls are shown on the left, and the effects of TPP8 and comparators on CFU reduction  
313 are shown after 3 days of treatment. As MIC measured in tubes can be different from those  
314 measured in 96-well plates, tube MICs were measured and used as the baseline in these  
315 experiments (11). They were as follows (with MIC values shown in Table 1 and determined by  
316 the microbroth dilution method in parentheses): TPP8, 0.04  $\mu$ M (0.02  $\mu$ M); SPR719, 6  $\mu$ M (1.5  
317  $\mu$ M); MXF, 6  $\mu$ M (3  $\mu$ M), CLR, 1.5  $\mu$ M (3  $\mu$ M). **(B)** To determine the activity against  
318 intracellular bacteria, THP-1 cells were prepared and differentiated into macrophages with  
319 phorbol-12-myristate-13-acetate for 24h, the resulting macrophages were infected with an MOI  
320 of 10 for 3h using *M. abscessus* ATCC19977 as described previously (26) and treated with the  
321 same concentration range of TPP8, SPR719, MXF, or CLR as in **(A)**. Intracellular CFU were  
322 enumerated by plating samples on agar Middlebrook 7H10 agar after 3 days of treatment.  
323 Experiments in **(A)** and **(B)** were carried out three times independently and the results are  
324 represented as mean values with standard deviations.

325

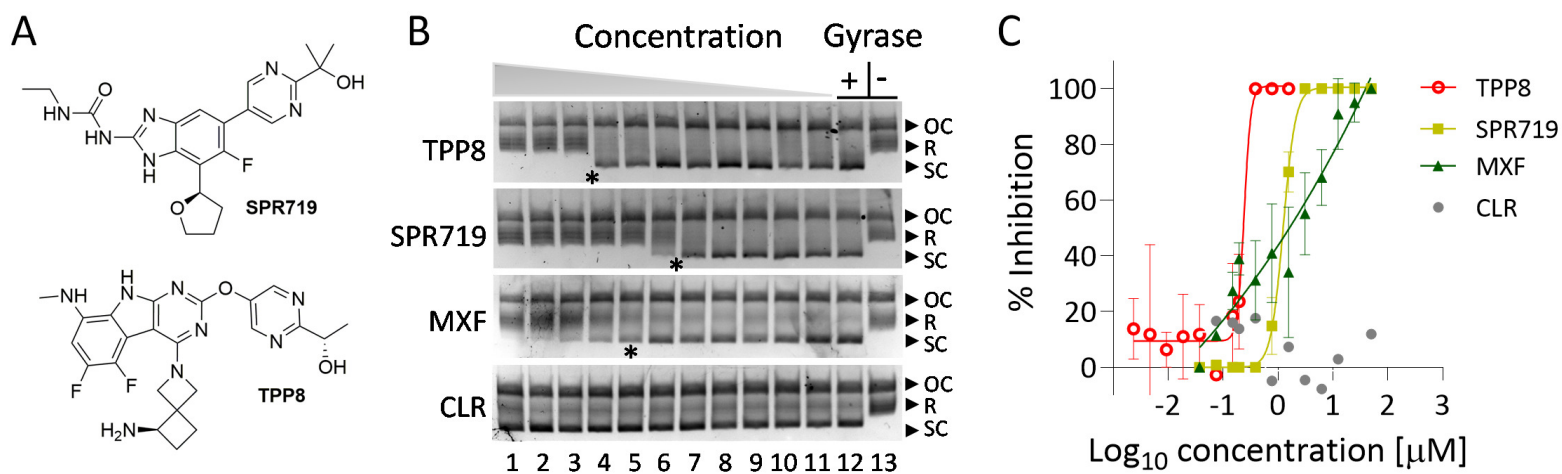
326 **Figure 3.** Pharmacokinetic profile and efficacy of TPP8 in mice. **(A)** Plasma concentration-time  
327 profile of TPP8 following a single intraperitoneal dose of 10 or 25 mg/kg in CD-1 mice. The  
328 MIC of TPP8 against *M. abscessus* K21 (Table 1), the strain used in our murine infection model,  
329 is indicated by a dotted line. **(B)** Efficacy of TPP8 and comparator compounds in a NOD SCID

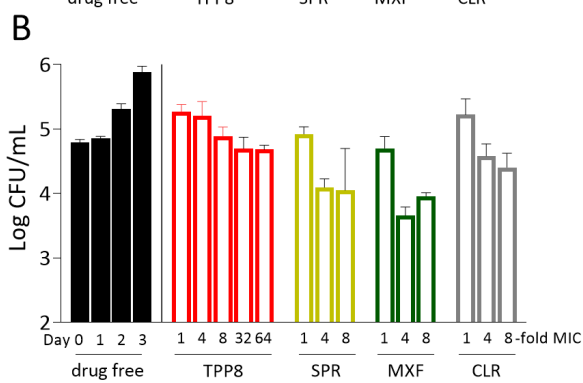
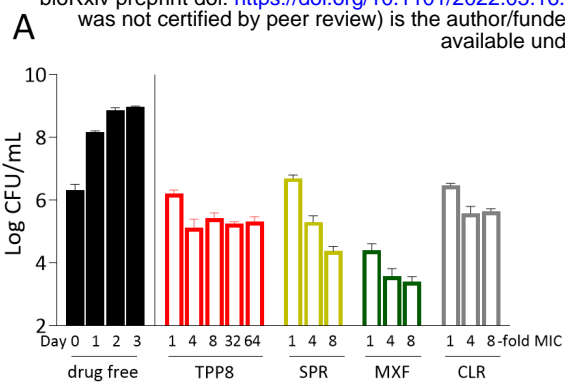


330 mouse model of *M. abscessus* K21 lung infection. Mouse lung and spleen CFU are shown one  
331 day after intranasal infection with *M. abscessus* K21 (D1), following daily intraperitoneal  
332 administration of 20% Solutol HS15 in PBS pH 7.4 (TPP8 vehicle) for 10 days (D11, DF: drug  
333 free), daily intraperitoneal administration of TPP8 (12.5 or 25 mg/kg), or daily oral  
334 administration of clarithromycin (CLR 250 mg/kg formulated in 0.5% carboxymethyl cellulose),  
335 moxifloxacin (MXF 200 mg/kg formulated in water) or SPR720 (SPR 100 mg/kg formulated in  
336 0.5% methylcellulose) for 10 days. Mean and standard deviation are shown for each treatment  
337 group (n=6). Statistical significance of the results was analyzed by one-way analysis of variance  
338 (ANOVA) multi-comparison and Dunnett's post-test: \*, p<0.01; \*\*, p<0.001. The experiment  
339 was carried out twice and one representative dataset is shown.

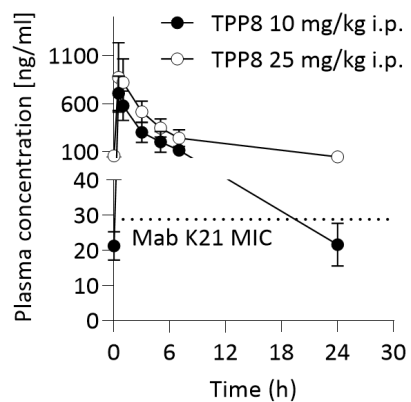
340

341





A



B

